

Potential of *Terminalia arjuna* as a Promising Phytoremedy Against COVID-19: DPPH Scavenging, Catalase Inhibition and Molecular Docking Studies

Senthilkumar Arumugam^a, Swati S. Dash^a, Kartik Mitra^b, Mukesh Doble^b and
Sathyanarayana N. Gummadi^{a*}

^aDepartment of Biotechnology, Bhupat and Jyoti Mehta School of Biosciences, Applied and
Industrial Microbiology Laboratory, Indian Institute of Technology Madras, Chennai, 600 036
India

^bDepartment of Biotechnology, Bhupat and Jyoti Mehta School of Biosciences, Drug Design
Laboratory, Indian Institute of Technology Madras, Chennai, 600 036 India

*Corresponding author

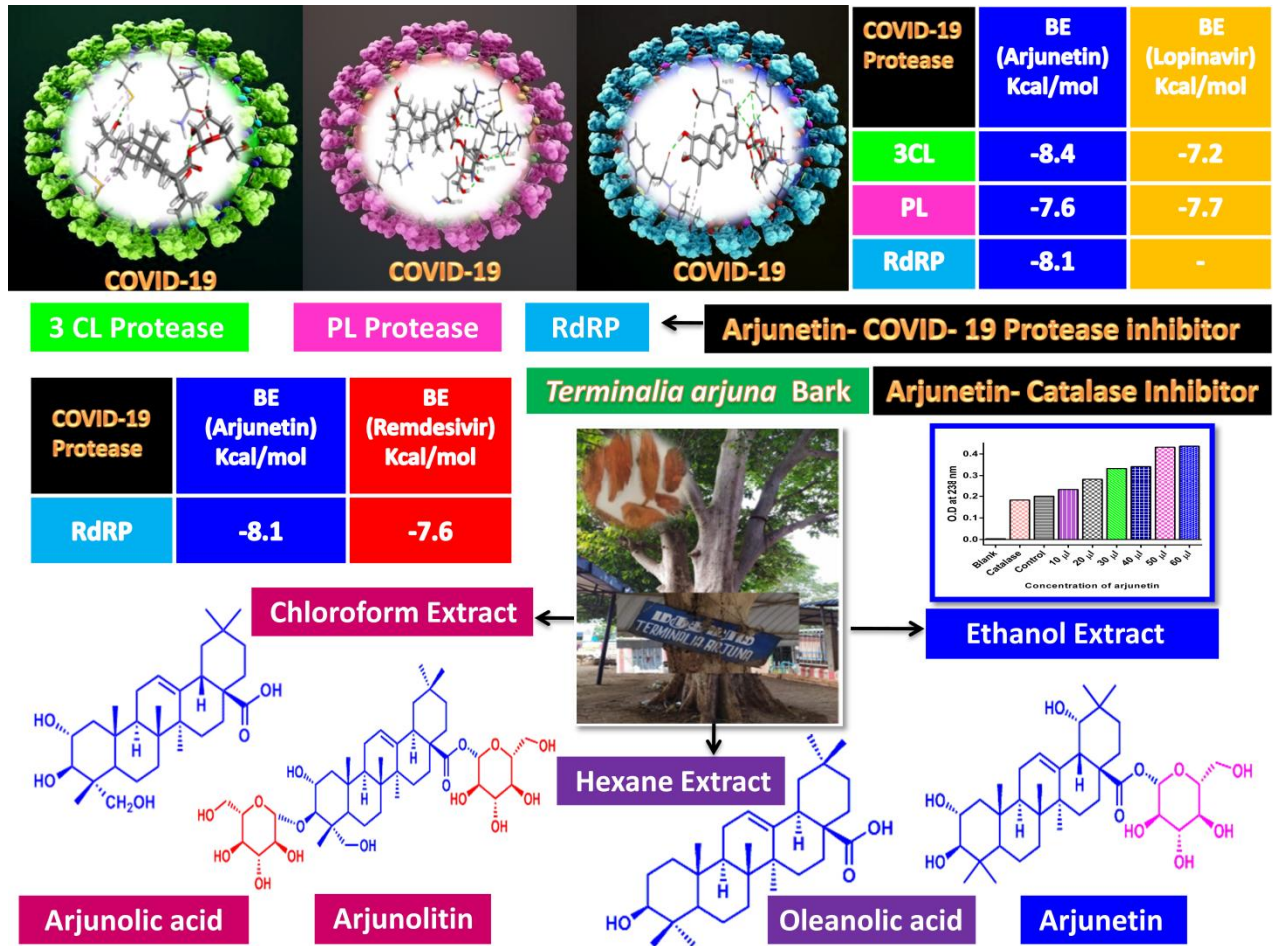
Phone: (+91)-44-2257-4114, Fax: (+91)-44-2257-4102, Email: gummadi@iitm.ac.in

ABSTRACT

Stem and bark of the tree *Terminalia arjuna* Wight & Arn. (Combretaceae) has been documented to exhibit therapeutic properties like cardiogenic, anticancer, antiviral, antibacterial, antifungal, hypocholesteremic, hypolipidemic and anti-coagulant. In previous studies, ethanolic extract of *T.arjunabark* effectively inhibited catalase activity along with demonstration of DPPH radical scavenging activity. Further, four known oleananetriterpenoids type compounds viz., oleanolic acid, arjunolic acid, arjunolitin, arjunetin were isolated from ethanolic bark extract and the structures of which were elucidated using ^1H , ^{13}C NMR, HR-ESIMS, IR and compared with literature data. Of the various compounds, Arjunetin showed significant inhibition of catalase activity as compared to the other compounds and most probably conferring antibacterial and antiviral property of the extract. In the present study, considering the currently on going viral pandemic of SARS-CoV-2 and the need for an effective antiviral agent, *T.arjuna* with its cardioprotective ability and inhibitory action against catalase presents to be a promising candidate against the virus. Molecular docking studies showed that arjunetin binds to protease of SARS-CoV-2 (3CL, PL and RdRP) and had higher binder energy values (3CL, -8.4 kcal/mol; PL, -7.6 kcal/mol and RdRP, -8.1 kcal/mol as compared with FDA approved protease inhibitor drugs lopinavir (3CL, -7.2 kcal/mole and PL -7.7 kcal/mole) and Remdesivir (RdRP -7.6 kcal/ mole). We conclude that there is profound evidence of arjunetin as a potential protease inhibitor of SARS-CoV-2 which is comparable to FDA approved antivirals Lopinavir and Remdesivir and can serve as a candidate for drug development against SARS-CoV-2.

KEY WORDS: *Terminalia arjuna*, DPPH scavenging, catalase inhibition, SARS-CoV-2, protease, arjunetin, molecular docking

Graphical abstract (TOC Graphics)



1. INTRODUCTION

The World Health Organization reported that infectious diseases caused by pathogenic microorganism account for about 25% of the total annual deaths that occur worldwide, both in developed as well as developing countries, the incidence being higher in developing nations¹. In the present time, drastic changes in climate and increasing levels of pollutants in the atmosphere result in accelerating the rate of genetic mutations in these microorganisms thereby increasing their infectivity. Climate change also increases the contact of insect vectors and animal reservoirs of pathogens with humans, resulting in emergence of new diseases which are unresponsive to available treatment regimes. Overuse of antibiotics also leads to emergence of multi-drug resistant strains that are hard to eliminate. Therefore, discovery of new and novel antibacterial and antivirals coupled with better understanding the mechanism of action is the present challenge in research.

In this aspect, plant derived phytochemicals can offer new direction in development of methods for disease control. Traditional systems of medicine such as Ayurveda, Siddha, or Unani have depended on natively available flora for treatment of almost all kinds of maladies since centuries. *Terminalia arjuna* (TA) (Family: Combretaceae), a tree native to Indian subcontinent, is extensively used in many of traditional forms of medicine for the treatment of hypertension and coronary heart diseases² earning it the epitaph of “Guardian of the heart”. It is known to confer cardioprotective properties such as strengthening heart muscles and improving functioning of cardiac muscles, thereby alleviating heart failure, angina and hypercholesterolemia. Stem and bark of this plant exhibits various other therapeutic properties such as expectorant, antidiarrhetic, purgative, laxative and have been also used to treat leucoderma, anaemia, hyperhidrosis, asthma and tumors³. In addition, it has also been reported that the bark of *T. arjuna* also possesses good anticancer, antiviral and antimicrobial activities⁴⁻⁶. It has been

hypothesized that the cardioprotective activity of TA bark extracts are likely by the activation of endogenous antioxidant molecules by triterpenes namely arjunolic acid.⁷⁻⁹ However, knowledge on the mode of action of the component in the bark/stem that confers antimicrobial activity is lacking in literature.

Previous studies carried on elucidation of properties of *T.arjuna* showed that catalase activity was inhibited by ethanolic bark extract *in vitro*.¹⁰ The enzyme catalase is one of the endogenous antioxidant defense systems that helps in decreasing accumulation of reactive oxygen by decomposing hydrogen peroxide during cellular metabolism to water and molecular oxygen. It is postulated that catalase activity protects pathogens from inactivation by reactive oxygen species (ROS) in eukaryotic systems, making it a potential virulence factor in many bacterial pathogens. Studies have shown that catalase facilitates intracellular survival of bacterial pathogens such as *Mycobacterium tuberculosis*¹¹, *Campylobacter jejuni*¹², *Helicobacter pylori*¹³ and Herpes Simplex Virus¹⁴. It has been also reported that increased serum catalase activity may also alter immune function, viral replication, and/or repair processes^{15,16}. In this regard, the catalase inhibitor in *T. arjuna* extract necessitates further research.

We believe *T. arjuna* stands as a strong contender for development of an effective therapeutic agent for the current pandemic respiratory disease, COVID-19 which emerged in December 2019 and has been spreading at a rapid rate all over the world with high rate of infectivity and mortality. The viral pathogen, SARS-CoV-2, appears to spread more efficiently, making it difficult to contain and increasing its pandemic potential^{17,18}. One of the important pathological aspect of COVID 19 is its effect on cardiovascular system and *T. arjuna* has well documented cardio protective properties, making it an excellent match. Catalase inhibition is another important aspect which has been shown to inhibit viral replication and spread. Literature shows

that bark extract of *T.arjuna* possesses anti-herpesvirus activity in inhibiting viral attachment and penetration and also disturbing the late event of infection¹⁹.

Consolidating information available from literature and experiments conducted in our lab on *T.arjuna* extracts, it is evident that *T.arjuna* can be regarded as an apt candidate in the search of antivirals against COVID-19. In this study, different solvent extracts of TA and the purified compounds from ethanol extracts have been evaluated for their effect on catalase activity. Also, molecular docking studies of isolated compound from ethanolic bark extract with have been carried out on protease of SARS-CoV-2. With no antivirals or vaccines developed till date for the epidemic, the present study will serve as a frontier for the much needed research on drug development for COVID-19.

2. RESULTS AND DISCUSSION

2.1 2, 2-Diphenyl-1-Picrylhydrazyl (DPPH) Free Radical Scavenging Assay

DPPH is a stable free radical used widely to study scavenging activities of antioxidants that can donate a hydrogen atom. The unpaired electron in DPPH becomes paired in the presence of a free radical scavenger (antioxidant) and the extent of decrease in DPPH absorption is proportional to the concentration of radicals scavenged, according to principle of Blois. This change in absorbance produced by this reaction forms the basis of tests to determine ability of compounds to act as free radical scavengers. In this study, the free radical scavenging property of *T. arjuna* bark, extracted in various solvents, was analyzed by UV-Visible spectroscopy and EPR spectroscopy as described below:

2.1.1 DPPH Assay with UV-Visible Spectrophotometer

Scavenging of DPPH radicals, which have maximum absorption at 519 nm in ethanol by antioxidants, results in a decrease in absorption over time which can be monitored using a UV-

visible spectrophotometer at room temperature. Scavenging capacity can be represented as % inhibition of DPPH radical. In this study, marked decline of the absorption intensity at 517 nm was observed after adding 10 μ l of *T.arjuna* bark extracted in various solvents (hexane, chloroform, ethyl acetate, acetone, ethanol and water) individually to DPPH solution. The results from different bark extracts were compared with that from ascorbic acid, a known antioxidant, at various time intervals (Figure 1a-f).The decrease in absorption could be attributed to the phytochemicals in the bark extracts which donates protons to DPPH and decolorize it.

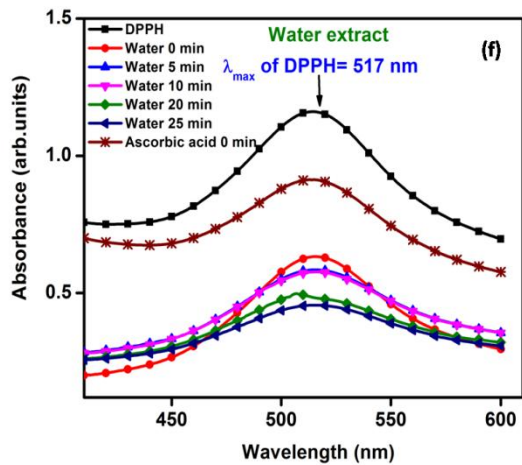
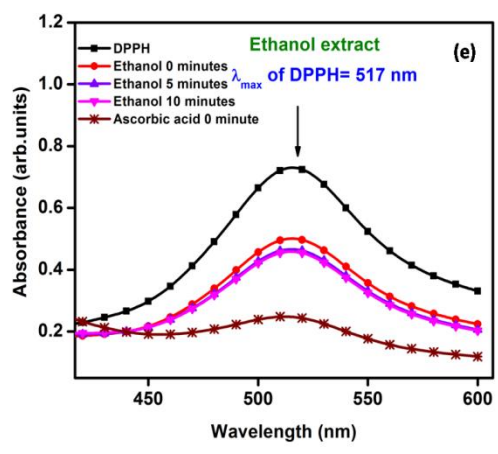
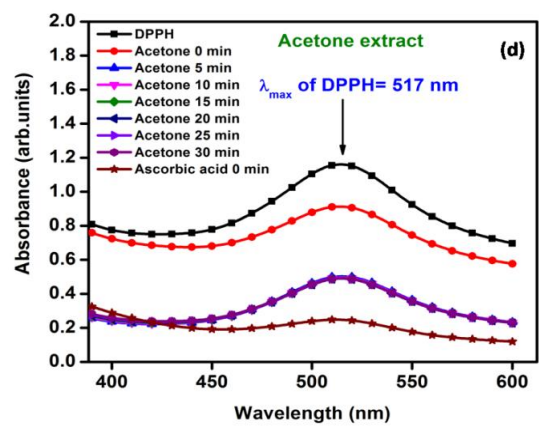
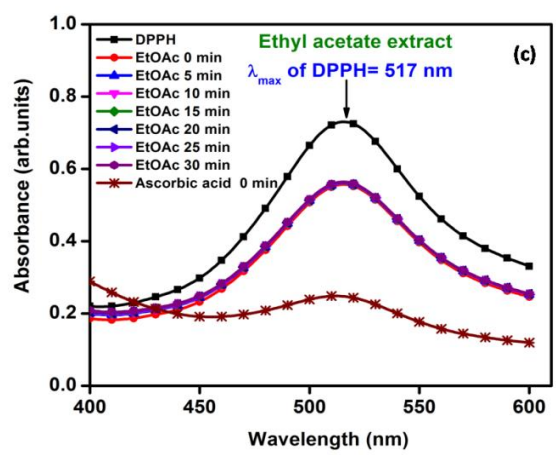
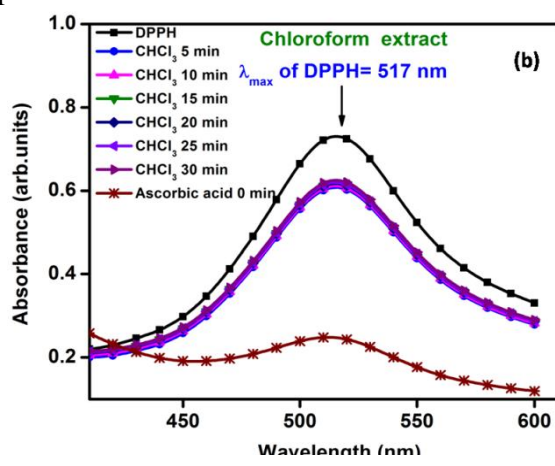
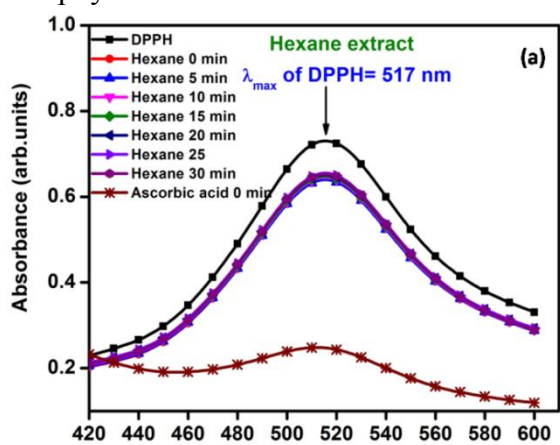


Figure 1. DPPH radical scavenging activity with different extracts by UV/vis (a) Hexane (b) Chloroform (c) Ethyl acetate (d) Acetone (e) Ethanol (f) Water.

It was found that the extracts varied significantly in terms of antioxidant activity. Ethanolic extract showed highest activity compared with other extracts which was equivalent to ascorbic acid, the standard antioxidant (Figure 2a and b) and Table 1. Percentage inhibition of DPPH radical scavenging activity at 5 minutes followed the order Ethanol > Acetone > ethyl acetate > Water > Chloroform > Hexane (Table 1).

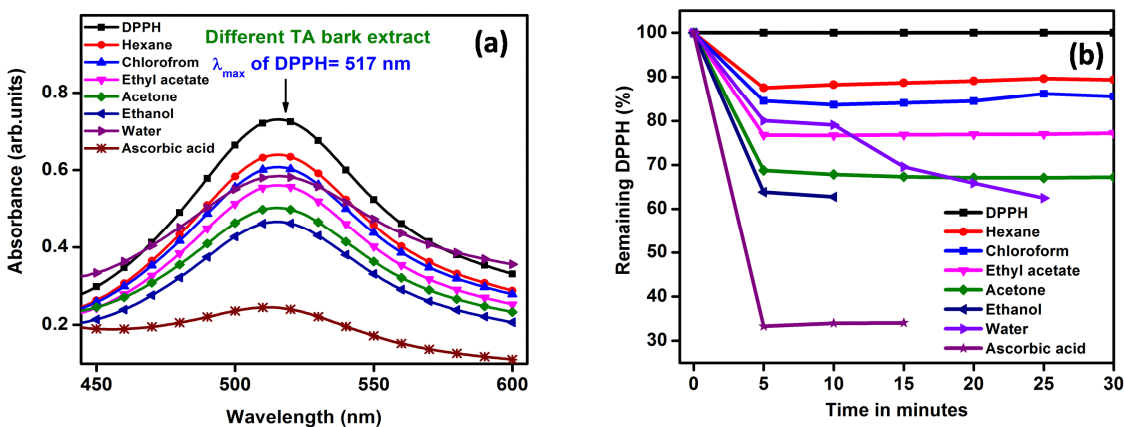


Figure 2. (a) Comparison of DPPH radical scavenging activity with different TA bark extract with DPPH and with standard (ascorbic acid) by UV/visible (b) Comparison % Inhibition for different TA bark extract with DPPH and with standard (ascorbic acid) by UV/vis spectrum

Table 1. % of inhibition of DPPH radical scavenging activity with different TA bark extract with DPPH and with standard (ascorbic acid).

Sl.No.	DPPH Scavenging activity % of inhibition (20 µl of each extract (1mg/mL))						
	Extracts	5 min	10 min	15 min	20 min	25 min	30 min
1	Hexane	12.41	11.69	11.27	10.86	10.31	10.56
2	Chloroform	16.79	16.29	15.39	15.48	15.13	14.40
3	Ethyl acetate	23.75	23.22	23.30	23.18	23.08	23.04
4	Acetone	31.24	32.16	32.67	32.92	32.93	32.78
5	Ethanol	36.18	37.25	-	-	-	-
6	Water	19.93	20.91	34.13	37.28		
7	Ascorbic acid	66.72	66.11	-	-	-	-

2.1.2 DPPH Assay with EPR Spectroscopy

EPR spectroscopy was used to quantify rate of DPPH radical disappearance in the presence of bark extract in this study. This technique has been used previously to assess free radicals scavenging ability of compounds^{20,21}. EPR determination of antioxidant activity is based on measuring the changes in the intensity of the EPR spectrum of stable radicals that result from their interaction with bark extracts antioxidants.

In this study, the EPR spectrum of ethanolic solutions of DPPH with various extracts was compared to the spectrum obtained from pure DPPH in order to study the decline in DPPH signal intensity, which indicated scavenging. Ethanolic solutions of DPPH were mixed with solutions of prepared bark extract and decline in DPPH signal intensity was monitored by EPR (Figure 3). Antioxidant activity (AA) of different extracts was measured based on remaining DPPH residue (%) and it was in the order of Hexane (77.10%)>Chloroform (76.25%)>Ethyl acetate

(74.95%)>Acetone (70.69%)>Ethanol (68.10%)> Water (65.23%) at 5 minutes. Based on above results antioxidant activity trends was observed in the order of Water>Ethanol>Acetone>Ethyl acetate>Chloroform>Hexane, the decrease in DPPH peak intensity observed to be highest in water and ethanol extract(Figure 4 and Table 2) indicating their superior antioxidant property as compared to extracts in other solvents. This is in correlation with previous studies^{22,23}.

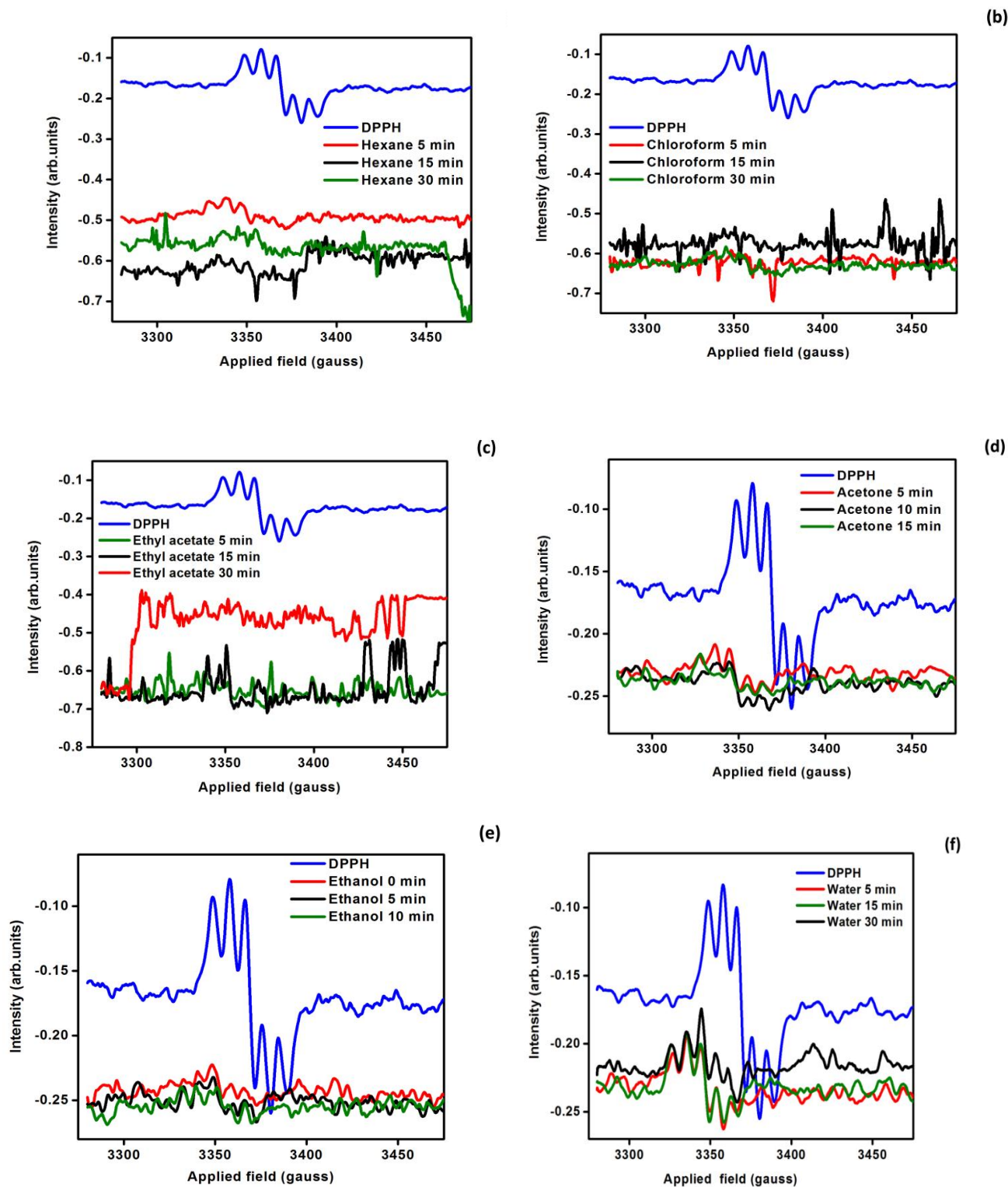


Figure 3.EPR spectra of DPPH with various extract (a) Hexane extract (b) Chloroform extract (c) Ethyl acetate extract (d) Acetone extract (e) Ethanol extract (f) Water extract.

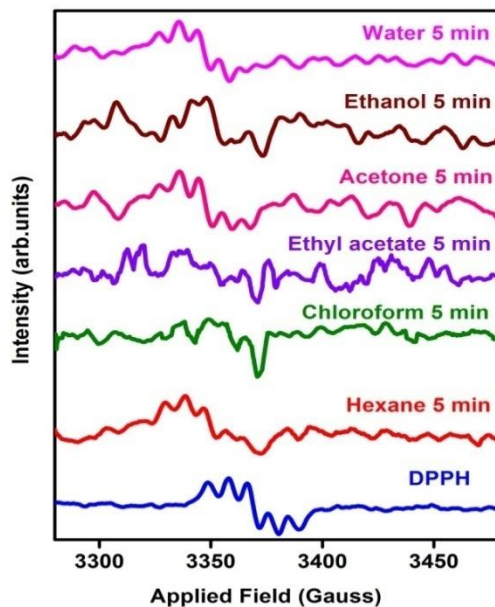


Figure4.Comparison of the EPR spectra of DPPH and different TA extract with DPPH at 5 min.

Table 2.Calculation antioxidant activity (AA) of different TA extracts using EPR

Antioxidant activity (AA) of different extracts				
Remaining DPPH Residue (%)				
	Time			
Extracts	0 min	5 min	10 min	15 min
Hexane	77.30	77.10	76.35	75.01
Chloroform	76.53	76.25	76.05	75.65
Ethyl acetate	75.36	74.95	73.20	72.85
Acetone	73.65	70.69	62.50	61.35
Ethanol	71.59	68.10	66.62	-
Water	66.66	65.23	64.76	63.41

2.2 Mechanism of DPPH with TA Extract

Polyphenolic compounds in TA extract are good reducing agents because of the hydrogen donor properties of their phenolic hydroxyl groups. When DPPH solution is mixed with TA extract, the phenolic compounds donate hydrogen atoms, thereby converting DPPH to its reduced form with a resulting decrease in absorbance at 517 nm.

Earlier studies on ethanolextraction, this type of triterpenoids glycoside compound revealed that certain structural features improve the efficiency in the trapping of DPPH radicals, such as hydroxyl groups and a ester glycoside, which increase the electronic delocalization in the molecule and it contributes to the stability of the produced radicals, resulting in an increase in the DPPH radical-scavenging capacity²⁴(Sanchez et al 2010)

The DPPH assay is based on both single electron transfer (SET) and hydrogen atom transfer (HAT) reactions. Antioxidants react with free radicals by different mechanisms hydrogen atom transfer (HAT) or single electron transfer mechanism (SET); or the combination of both HAT and SET mechanisms. Details of the mechanism have been given in the supplementary section (Figure S1). Ethanol extract from *T.arjuna* has the proton-donating capacity and could serve as inhibitor of free radical and probably as a primary antioxidant^{25,26}. Considering the obtained results, TA ethanol extract showed a potent antioxidant activity as indicated by the scavenging ability observed against DPPH radicals.

2.3. Isolation and Structure Elucidation

4 different compounds were isolated from TA extracts and were identified using IR spectrum studies, ¹³C NMR and ¹H NMR. Compounds 1, 2 and 3 were identified asoleanoic acid, arjunolic acid and arjunolitin. Details of all spectrophotometric data have been provided in the supplement section (Figures S2-S4).

Compound 4 was obtained as colorless solid from ethanol fraction using 100% methanol as eluent. It showed UV λ_{max} (methanol) 423nm. It exhibited characteristic IR absorption bands trisubstituted double bonds (1630 cm^{-1} , 894 cm^{-1}), hydroxyl (3355 cm^{-1}), ester (1730 cm^{-1}), methyl (1452 cm^{-1}), gem dimethyl 1391 cm^{-1} , C-O stretching frequency ($1260, 1161, 1049\text{ cm}^{-1}$). On the basis of mass and ^{13}C NMR spectra the molecular ion peak of 4 was determined at $m/z 673.4$ $[\text{M}+\text{Na}]^+$ $\text{C}_{36}\text{H}_{58}\text{NaO}_{10}$, $m/z 689$ $[\text{M}+\text{K}]^+$, $m/z 511$ $[\text{M}-162]^+$, $m/z 527$ $[\text{M}-162-44]^+$, $m/z 430$ $[\text{M}-162-44-34]^+$, $m/z 413$ $[\text{M}-162-44-41]^+$ supported one glycoside, three removable hydroxyl group and one ester function in the molecule.

^1H NMR spectrum of compound (4) exhibited signals of an olefinic proton at $\delta_{\text{H}} 7.0$ (1H, brs, H-12) and seven methyl singlet's δ_{H} (0.12, 0.16, 0.19, 0.33, 0.36, 0.40, 0.57, 7XCH_3 , 21H), the spectrum showed three oxygen bearing methine protons at $\delta_{\text{H}} 4.47$ (1H, brs, H-19), $\delta_{\text{H}} 4.66$ (1H, s, H-3 α), $\delta_{\text{H}} 4.73$ (1H, d, $J= 9.5$ Hz, H-2 β), $\delta_{\text{H}} 3.48$ (1H, brs-H18), $\delta_{\text{H}} 3.32-3.89$ (glucose hydrogen's). ^{13}C NMR spectrum displayed 36 signals inclusive of seven methyl signals δ_{C} (13.9, 16.9, 17.0, 17.6, 23.5, 25.8, and 27.3), three secondary hydroxyl groups δ_{C} 69.7 (C-2), 75.6 (C-3), 77.9 (C-19), one trisubstituted double bond δ_{C} 121.8 (C-12), 144.2 (C-13), ester carbonyl δ_{C} 175.4 (C-28), glucose carbon δ_{C} 60.2, 60.8, 67.6, 72.5, 76.8, 94.26. The anomeric proton signals at $\delta_{\text{H}} 6.8$ (1H, -H1') in the ^1H NMR spectrum and anomeric carbon signals at $\delta_{\text{H}} 94.2$ in the ^{13}C NMR spectra of compound attributed to a β -glucose unit linked to the C₂₈ carbonyl group of the genin through an ester bond^{4,27,28}. From the above all spectroscopic data the compound 4 was named as arjunetin.

Previous results showed that ethanolic extract had significantly higher antioxidant ability compared to extracts from other solvents. Since arjunetin is the identified phytochemical in the ethanol fraction it may have higher therapeutic significance as compared to other compounds

isolated and identified. This is further confirmed in our studies on catalase inhibition as described in the next section.

2.4. Catalase Assay with Arjunetin (Compound4) from Ethanol Extract of TA Bark

Different bark extracts of *T.arjuna* showed inhibition of catalase activity. Amongst the all the extracts least inhibition was noted with chloroform extract and maximum inhibition was observed with ethanol extract(Figure 5). Dose dependent studies of isolated arjunetin molecule from ethanolic bark extract on catalase activity showed that inhibitory effect increased with increasing concentration of arjunetin (Figure 6).This is in contrast with previous findings where it has been observed that ethanolic bark extracts enhanced the catalase levels *in vivo* in ischemic

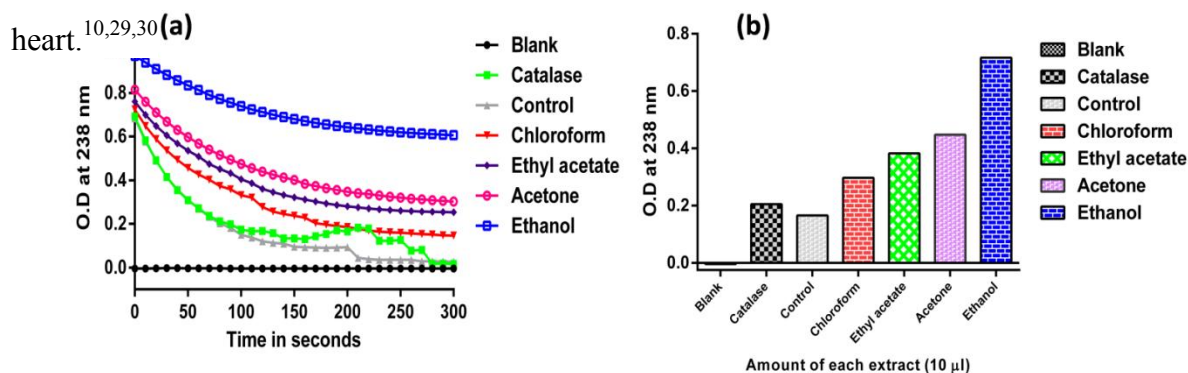


Figure 5:Effect of *T. arjunabark* extracts on catalase activity. (a) Comparison of catalase activity with different *T. arjunabark* extract. (b) Bar graph of comparison of catalase activity with different *T. arjunabark* extract.

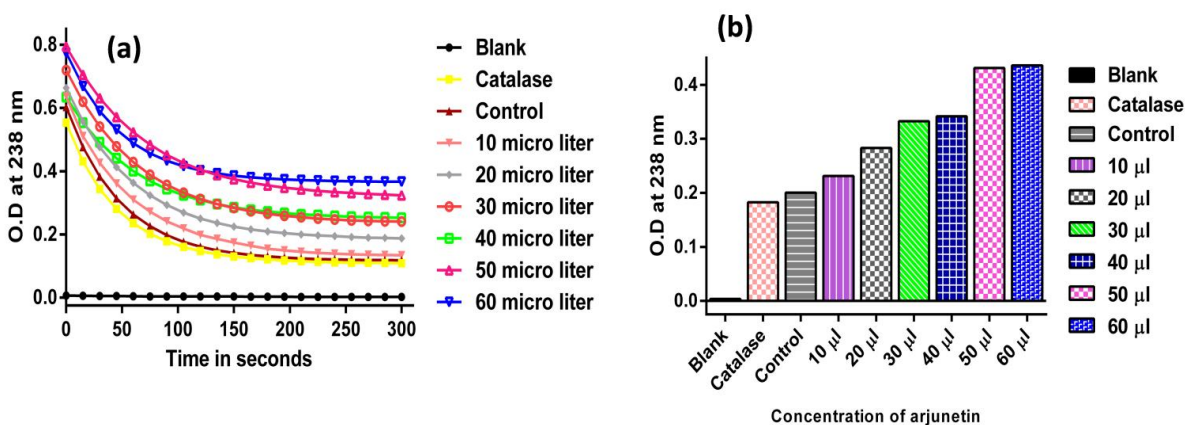


Figure 6:Effect of arjunetin from ethanol extract of *T. arjunabark* on catalase activity (a) Comparison of catalase activity with different amounts of arjunetin. (b) Bar graph of comparison of catalase activity with different amounts of arjunetin

The binding efficiency is attributed to the hydroxyl groups and ester glycoside present in arjunetin, which serve as hydrogen bond donors. Involvement of positive charge on the carbon atom of the ester bond with the electronegative groups of amino acid residues like histidine also contributes towards efficient binding. Here it can be reasoned that at this concentration of arjunetin it can also bind to other non-specific targets *in vivo* due to the presence of OH groups.

Catalase is an antioxidant oligomeric enzyme (MW =2,40,000) with four identical subunits arranged tetrahedrally. In eukaryotes it plays an important role in protecting cells from oxidative damage due to ROS. However, in certain bacteria and viruses, catalase is present as avirulent factor and is very important for the intracellular survival of the pathogen and disease progression. In this regard, compounds that bind to catalase and elicit enzyme inhibition can act as efficient antimicrobial and antiviral agents. It is known that inhibitor 3-AT (an efficient inhibitor of catalase) binds with histidine residue (His75) near heme group of catalase forming a non-coplanar adduct (very close to Tyr358). Loss in activity of catalase suggests involvement of arjunetin cation with histidine anion ($pK_a=6.5$) near tyrosine residue (Tyr358) of active site. This information can be used in *in-silico* methods of drug development using arjunetin.

In the present study, physiological changes have been demonstrated by inhibition of catalase by arjunetin. From the decay curves as shown in Figure 6, it is inferred that the rate of H_2O_2 degradation is reduced by arjunetin, proving arjunetin to be a good catalase inhibitor and therefore has potential to be studied for the development of an effective antibiotic.

SARS-CoV-2, the virus behind COVID-19 has no cure till date. Two main pathophysiologies of this disease is its effect on cardiovascular system and the development of adult respiratory

distress syndrome (ARDS). Studies have shown that serum catalase activity increases in septic patients with ARDS³¹. Considering the cardioprotective nature of *T.arjuna* and the ability to inhibit catalase, there is immense promise in this molecule for further research and use in development of an effective cure against SARS-CoV-2.

2.6. Inhibition of SARS-CoV-2 Protease by Arjunetin: Molecular Docking Studies

Since the appearance of COVID-19 pandemic, researchers all over the world have been proactively searching for a cure. Remdesivir was used in the first case of COVID-19 during January 2020 in Washington. Remdesivir, the single Sp isomer of the 2-ethylbutyl L-alanine phosphoramidate prodrug, has been reported to inhibit COVID-19 virus proliferation and therefore has clinical potential. FDA approved HIV protease inhibitors such as lopinavir and ritonavir have been reported to be active against SARS and MERS. Clinical trials have been initiated to test HIV protease inhibitors such as lopinavir and ritonavir in patients infected with novel coronavirus SARS-CoV-2.

In addition, natural compounds purified from plants can prove to be effective against the virus. Several plant-based treatment strategies against viral infections have been well elucidated in traditional medicine, many of which have the potential to be evaluated for COVID-19³².

Since it may take a long time to come up with a concrete remedial measure, use of *in-silico* tools will be beneficial in short listing candidate molecules for further research. In-silico screening of natural compounds using molecular docking have already been carried out on numerous listed plant derived compounds with an aim to create a library for reference and research (Joshi et al., 2020). It was of our interest therefore to study inhibition of SARS-CoV-2 proteases by arjunetin, the bioactive component isolated from *T.arjuna*, via molecular docking. Lopinavir and ritonavir have been used as control for our study^{33,34}.

In this study, molecular docking of arjunetin was performed against SARS-CoV-2 3CL-protease, PL-protease and RNA-polymerase. Lopinavir was used as reference control for proteases. In case of 3CL-protease Arjunetin has better binding energy (-8.4Kcal/mol) compared to lopinavir. (-7.2 kcal/mol)(Figure 7). In case of arjunetin the interactions are predominantly hydrophobic contributed by LEU 141 and 27, whereas in case of lopinavir it was hydrophilic. In case of PL-protease, Arjunetin binding score (-7.6Kcal/mol) is similar to Lopinavir (-7.74 kcal/mol) (Figure 8) the binding score of Arjunetin towards SARs-CoV-2 RdRP polymerase was found to be -7.8 kcal/mol. Similarly, the binding score of SARs-CoV-2 RdRP with Remdesivir was found to be -7.6 kcal/ mole (Figure 9), thereby indicating that arjunetin might preferably inhibit 3CL-protease as compared to PL-protease and RNA polymerase and better binding energy values as compared to Remdesivir, Lopinavir (Table 3& 4). These results, combined with the previously elucidated antioxidant and catalase inhibitory properties of arjunetin make it a promising plant compound to be further evaluate against COVID-19.

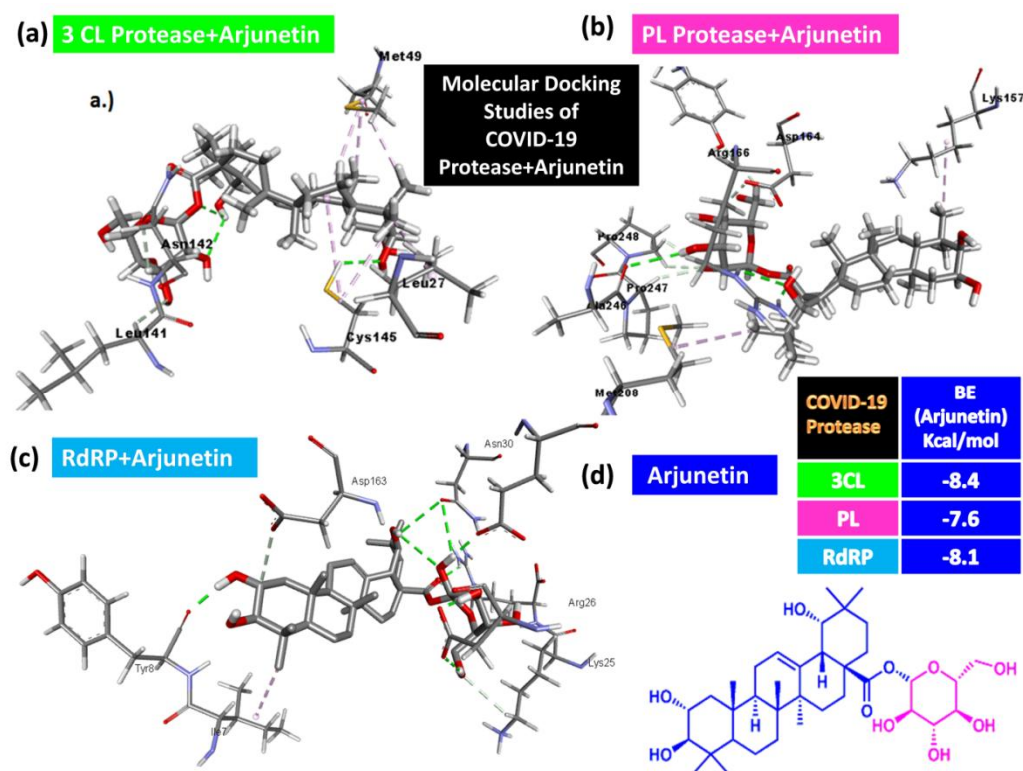
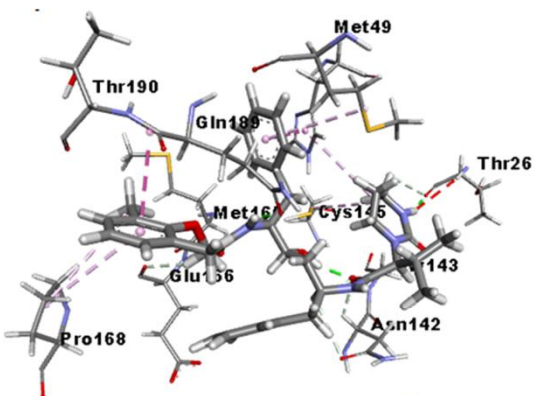


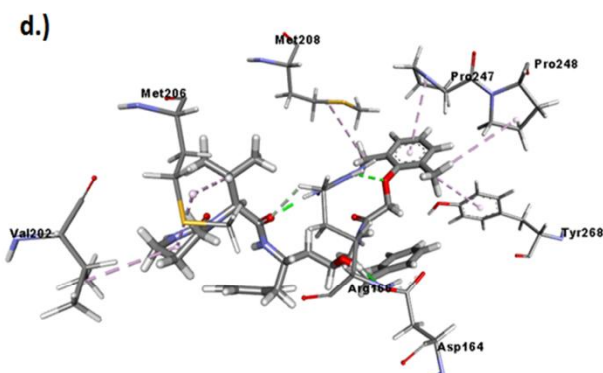
Figure 7: Molecular docking studies of SARS-CoV-2 protease with arjunetin (a) 3D interaction of 3CL+ arjunetin (b) 3D interaction of PL+ arjunetin, (c) 3D interaction of RdRP with arjunetin (d) Structure of arjunetin and binding energy values of SARS-CoV-2 protease with arjunetin.

**Molecular Docking Studies of COVID-19
Protease+Lopinavir**

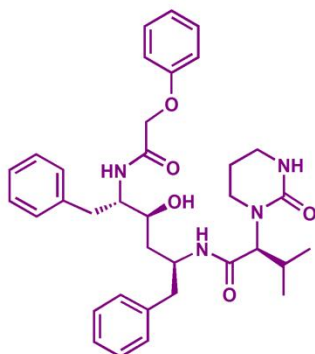
(a) 3 CL Protease+Lopinavir



(b) PL Protease+Lopinavir



(c) Lopinavir



(d)

COVID-19 Protease	BE (Arjunetin) Kcal/mol	BE (Lopinavir) Kcal/mol
3CL	-8.4	-7.2
PL	-7.6	-7.7
RdRP	-8.1	-

Figure 8: Molecular docking studies of SARS-CoV-2 protease with Lopinavir (a) 3D interaction of 3CL+Lopinavir, (b) 3D interaction of PL+ Lopinavir, (c) Structure of Lopinavir (d) Binding energy values of SARS-CoV-2 protease with Lopinavir

Molecular Docking Studies of COVID-19 Protease+ Remdesivir

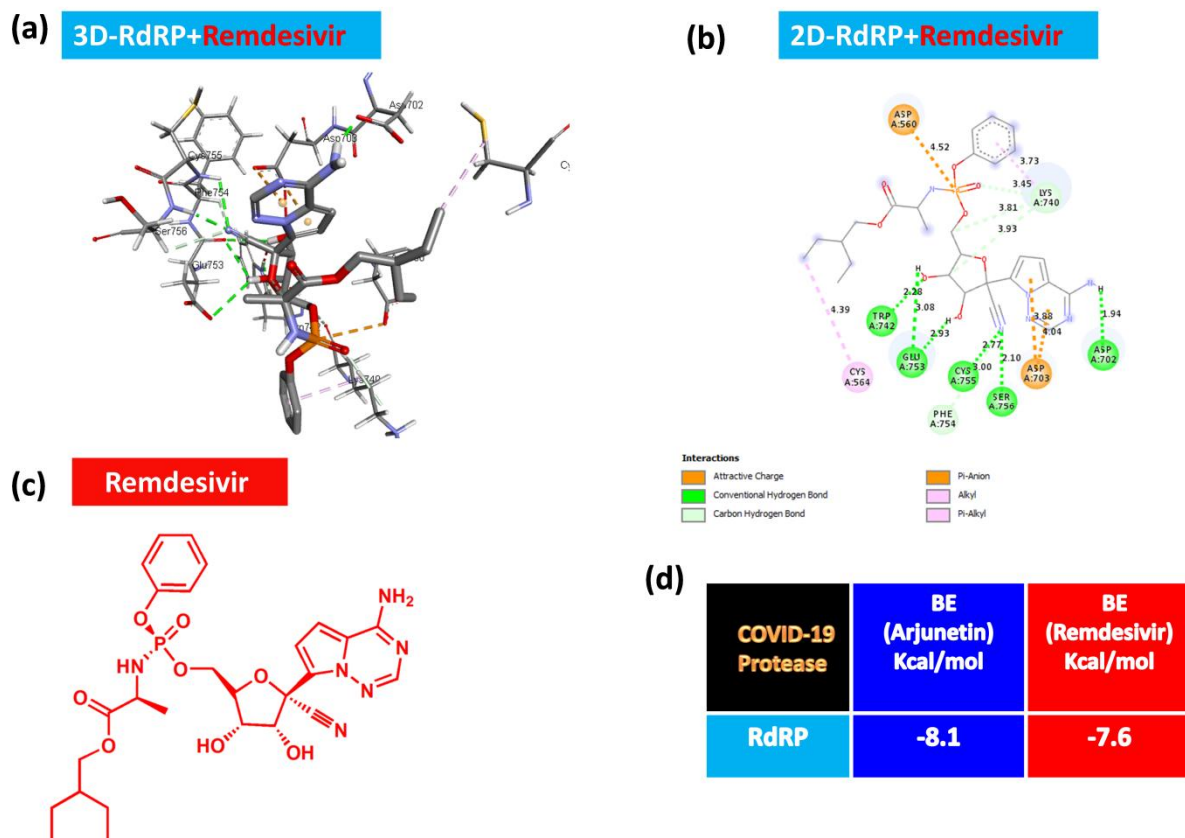


Figure 9: Molecular docking studies of SARS-CoV-2 protease RdRP with remdesivir a) 3D interaction of RdRP with remdesivir b) 2D interaction of RdRP with remdesivir v) Structure of remdesivir d) Binding energy values of SARS-CoV-2 protease RdRP with remdesivir

Table 3: Comparison of binding energy values of SARS-CoV-2 proteases 3CL, PL and RdRP with arjunetin, lopinavir and remdesivir.

COVID-19 Protease	Binding Energy (K cal/mol)		
	Arjunetin	Lopinavir	Remdesivir
3CL	-8.4	-7.2	-
PL	-7.6	-7.7	-
RdRP	-8.1	-	-7.6

Table 4:Key interaction of antivirals with amino acids in SARS-CoV-19 proteases; 3CL, PL and RdRP with arjunetin, 3CL and PL with Lopinavir andRdRP with Remdesivir.

Molecules	3CL-protease	PL -protease	RdRP
Arjunetin	Leu141, Leu27, Cys145, ASN12 and Met49	Pro248, Met208, Pro247,and Lys157	ARG26, Lys25, Asp160, Glu34, ASN30, Asp163, Tyr8, ILE 7
Lopinavir	Met 49, Pro168, ASN142, Cys145, Th190 and Thr 26	ASP164, Pro248, Met206, Val202, Tyr 260	-
Remdesivir	-	-	Asp560, Lys 740, Cys564, Trp742, Glu753, Cys755, Phe754, Ser756, Asp 703

3. CONCLUSIONS

The present study was carried out to identify and evaluate active components in solvent extracts of *T.arjuna* bark samples, which is known for its cardioprotective and antimicrobial properties. Ethanolic extracts had significantly higher free radical scavenging ability as compared to other extracts, indicating their antioxidant nature. Further the purified compounds arjunetin from ethanolic bark extract showed dose dependent inhibition of catalase activity *in-vitro*. Molecular docking studies on arjunetin against three proteases of SARS-CoV-2 viz. 3CL, PL and RdRP demonstrated that arjunetin can bind more efficiently to the viral proteases as compared to known commercially available antivirals thereby acting as inhibitor. We conclude that *T.arjuna* and its phytochemicals, particularly arjunetin, show promise as potential antiviral agents and can be utilized for further innovation and development of antiviral treatment regime against COVID-19.

4. METHODS

4.1. Collection of Plant Materials. The dry stem bark of *Terminalia arjuna* was obtained from Centre of Traditional Medicine and Research (CTMR), Chennai, India and collected from Pillaiyarpattai, Sri Karpagam Vinayager Temple thalaviruksha, Sivagangai District, Tamil Nadu, India and authenticated at Siddha Central Research Institute, Arumbakkam, Chennai, Tamil Nadu, India (voucher specimen no: T19081901A).

4.2. Chemicals and Reagents

Bovine serum catalase (CAS Number. 9001-05-2) and DPPH (2,2-Diphenyl-1-picryl hydrazyl radical) CAS Number 1898-66-4 was obtained from Sigma Aldrich, USA. Silica gel (230-400 mesh) and Sephadex LH-20 column obtained from Merck India and GE Healthcare, India respectfully. All the solvents used for extraction were AR grade procured in India. Ethanol (95% v/v technical grade) was purchased from Hayman, India.

4.3. Preparation of the Crude Extract. Air dried and finely powdered *T. arjuna* bark (75g) was extracted using Soxhlet apparatus with various solvents for 72 h using sequential refluxing with solvents of increasing polarity hexane (100mg), chloroform (400 mg), ethyl acetate (240mg), acetone (3g), ethanol (12g) and water (3g). After filtration and evaporation of solvents under vacuum, the residues were stored under room temperature. Phytochemical tests were carried out to detect presence of tannins, alkaloids, reducing sugars, saponins, flavanoid. Extracts of ethyl acetate, acetone, and ethanol had more tannins and extracts of hexane, ethyl alcohol and ethyl acetate were rich in flavonoid as reported in previous paper.¹⁰

4.4. Extraction and Isolation of Compounds from *T. arjuna* Bark. 1.5 kg of air dried bark of TA was ground to fine powder and sequentially extracted with solvents of increasing polarity

(hexane, chloroform, and ethanol each solvent 5L) for 72 h using Soxhlet apparatus. After filtration, evaporation was done under vacuum and the residues were stored at room temperature. A glass column (60cm X 50 mm) packed with silica gel (60-120 mesh) was used as stationary phase for the separation of phytochemicals in solvent extracts. Hexane fraction (10g) was eluted by column chromatography over silica gel(60-120 mesh) using varying concentration of chloroform in hexane as eluent (0-100% chloroform) to afford two fractions one at hexane-chloroform(9:1)to yield the mixture of compounds and at (1:1) to yield compound **1**(50 mg).Chloroform fraction (55g)was subjected to chromatography on silica gel eluting with hexane-EtOAc-methanol gradient to afford five fractions A-E.Fraction C (4:1, ethylacetate:hexane) was further purified by preparative TLC using CHCl_3 as solvent to yield the compound **2** which was pale yellow in color (500 mg).Fraction D (4:1,ethylacetate:methanol) was purified to obtain compound **3** as pale yellow colour powder (50 mg). Ethanol fraction (4g) was column chromatographed over Sephadex LH 20 using various concentration of methanol and water as eluent at 100% methanol to afford compound **4**as white crystalline solid (10 mg). The detailed scheme is given in supplementary material (Figure S5).

4.5.Analytical Techniques. UV spectra were recorded on a Jasco V 550 UV-VIS spectrophotometer. IR spectra were recorded on a Perkin Elmer spectrum one Fourier Transform Infrared spectrometer with KBr pellets. ^1H and ^{13}C NMR spectra of compounds were recorded on a JEOL 400 MHz NMR spectrometer in CDCl_3 with TMS as internal standard and with chemical shifts (δ) reported in ppm. HRESIMS were measured on a Q-TOF micro mass spectrometer (Waters USA) in positive ion mode with methanol as solvent. Operating parameters of Varian E112 EPR spectroscopy instrument were as follows: Frequency: 9.23 Hz,

Microwave Power: 10 mW Mod. Constant: 3.2 G-Time Constant: 0.5 Center Field: 3300 G-Scan range: 2000. All scans and sample positions were carried out with the same conditions.

4.6. Free Radical Scavenging Assay Using UV-Visible Spectroscopy. The antioxidant capacities of *T.arjuna* extracts were evaluated by measuring their free radical abilities to 1,1-diphenyl-2-picryl hydrazyl (DPPH) stable radicals following established procedure by measuring absorbance of 3 ml of 100 mM DPPH (ethanolic solution) that contained 20 µl of extract (1 mg/ml each extract). Ethanolic solution of 100 mM DPPH was taken as the blank³⁵. The disappearance of DPPH colour was measured spectrophotometrically at 517 nm (Jasco V 550 UV-VIS, Tokyo, Japan). Inhibition of free radical DPPH in percent (%) by following formula

$$\text{Inhibition (\%)} = 100 \times \frac{(A_{\text{blank}} - A_{\text{sample}})}{A_{\text{blank}}}$$

where, A_{blank} is the absorbance of DPPH solution without extract and A_{sample} is the absorbance of the tested extract.

4.7. Free Radical Scavenging Assay Using EPR spectroscopy

EPR spectroscopy was used to monitor the scavenging of DPPH radical by the TA extracts. 20 µl of TA extracts were mixed with 100 µl of methanolic solution of DPPH to a total volume of 3 ml and the EPR spectrum was measured using VARIAN E-112 ESR spectrometer at different time points. 3 ml of 100 mM DPPH in ethanol was taken as blank. The decrease in the intensity of DPPH peak, which was indicative of decrease in the concentration of DPPH radical, was monitored by EPR spectrometer for a period of 30 minutes during which the radical was stable³⁶. The DPPH radical was generated in ethanol solution and considered as a control (Figure S6). The DPPH radical scavenging activity was estimated as a ratio of individual DPPH signal peak height to that of control.

DPPH radical scavenging activity

$$1- \frac{(A \text{ of Sample})}{(A \text{ of Control})}$$

The DPPH radical scavenging activity of each sample was calculated by comparison of relative peak height for control (sample free) DPPH solution. DPPH radical reducing activity of each test sample was expressed as the percentage of DPPH residue

4.8. Catalase Assay. Catalase decomposes hydrogen peroxide molecules into water and oxygen.

The principle of the assay is that loss of the substrate measured at 238 nm until the substrate concentration becomes limiting. The assay was performed at 25°C using 50 mM sodium phosphate buffer of pH 7.0 containing 12 μM of H_2O_2 as substrate and 0.2 $\mu\text{g mL}^{-1}$ of bovine liver catalase. The absorbance was monitored at 238 nm as a function of time for 5 min. One unit of catalase activity is defined as the amount of enzyme required to break one micromole of substrate per minute. Measuring the absorbance of reaction mixture at 238 nm for 5 min monitored the activity of catalase. When the reaction proceeds, absorbance at 238 nm starts decreasing due to reduction of substrate concentration. The assay mixture contained 10 μg of extracts, 63 μl of 0.132 M hydrogen peroxide, 70 μl of 0.002 mg/ml catalase and the volume was made up to 700 μl with 50 mM phosphate buffer at pH 7.0. Assay with equal volume of corresponding solvent instead of extracts was used as blank. Similarly, Catalase assay was performed with compound 4 from ethanol extract with increasing concentrations within the range of 10 μg – 50 μg with the same conditions as described above. All the experiments were performed at least three times and the values mentioned are mean values within $\pm 5\%$ standard error.

4.9 Molecular Docking Studies. Molecular Docking studies were performed using UCSF Chimera and AutoDock Vina. The targets 3CL Pro (PDB-6lu7), PL-Pro and RNA-polymerase (PDB:6M71) were prepared for docking by adding hydrogen, assigning charges and removing water molecules using the dock prep module. The compound, which was to be docked, was minimized using AMBER forcefield and then docked using Autodock Vina. For 3CL-Pro, grid box of size 27*27*27 centered at coordinates (-16.1115, 12.1099, 66.6681) was made and docking was performed, That of PL-Pro grid box of size 29*29*29 centered at coordinates (-1.84143, 0.0274012, 1.57883) was made and docking was performed. For RNA polymerase the grid box of 35*29*30 centered at coordinates (-1.84143, 0.0274012, 1.57883). The pose with the lowest binding energy was considered as the best pose and saved for further study.

AUTHORS

Senthilkumar Arumugam-Applied and Industrial Microbiology Laboratory, Bhupat and Jyoti Mehta School of Biosciences, Indian Institute of Technology Madras, Chennai, 600 036 India.
Email:senthilorganic@gmail.com

Swati Sucharita Dash-Applied and Industrial Microbiology Laboratory, Bhupat and Jyoti Mehta School of Biosciences, Indian Institute of Technology Madras, Chennai, 600 036 India.
Email:swati.121@gmail.com

Kartik Mitra- Bioengineering and Drug Design Lab, Department of Biotechnology, Bhupat and Jyoti Mehta School of Biosciences, Indian Institute of Technology Madras, Chennai, 600 036 India.
Email:kartik.mitra.v@gmail.com

Mukesh Doble-Bioengineering and Drug Design Lab, Department of Biotechnology, Bhupat and Jyoti Mehta School of Biosciences, Indian Institute of Technology Madras, Chennai, 600 036 India. (+91)-44-2257-4107, Fax: (+91)-44-2257-4102.
Email:mukeshd@iitm.ac.in

Sathyanarayana N. Gummadi-Applied and Industrial Microbiology Laboratory, Bhupat and Jyoti Mehta School of Biosciences, Indian Institute of Technology Madras, Chennai, 600 036 India.
Email:gummadi@iitm.ac.in

CONTRIBUTION TO RESEARCH

SNG contributed to supervision, experimental design, methodology, bioassay and manuscript editing.

SA contributed to structural elucidation, data analysis, bioassay and manuscript writing.

SSD contributed to data analysis and manuscript writing

MD and KM contributed to the docking studies.

All authors contributed to the review of the final the manuscript.

CONFLICTS OF INTEREST

The authors declare that they have no conflict of financial interest

ACKNOWLEDGMENT

The authors are deeply grateful for financial support provided by IDRP, Department of Biotechnology, IIT Madras. The authors gratefully acknowledge Dr. Sreevidya Narasimhan, CDRI, Lucknow. The authors wish to thank the SAIF, Department of Chemistry, IIT Madras for EPR, FT- IR, NMR, and ESIMS facility.

REFERENCES

1. WHO. The evolving threat of antimicrobial resistance: Options for action. *Switzerland: WHO, 2012.*
2. Dwivedi, S.; Chopra, D. Revisiting *Terminalia arjuna* –An ancient cardiovascular drug. *J Tradit. Complement. Med.* **2014**,*4*, 224-231.
3. Jain, S.; Yadav, P.P.; Gill, V.; Vasudeva, N.; Singla, N. *Terminalia arjuna* a sacred medicinal plant, phytochemical and pharmacological profile. *Phytochem. Rev.* **2009**, *8*, 491-502.

4. Tripathi, V.K.; Singh, B. *Terminalia arjuna*- its present status (a review).*Orient. J. Chem.***1996**, *12*, 1-16.
5. Cooper, E.L. CAM, eCAM, Bioprospecting: the 21st century pyramid.*Evid. Based. Compliment. Alternat. Med.* **2005**, *2*,125-127.
6. Patil, U. H.; Gaikwad, D.K. Phytochemical evaluation and bactericidal potential of *Terminalia arjunastem* bark.*Int. J. Pharm. Sci. Res.***2011**,*2*, 614-619.
7. Sumitra, M.; Manikandan, P.; Kumar, D.A.; Arutchelvan, N.; Balakrishna, K.; Manohar B. M.; Puvanakrishnan, M. Experimental myocardial necrosis in rats: role of arjunolic acid on platelet aggregation, coagulation and antioxidant status. *Mol. Cell Biochem.***2001**, *224*, 135-42.
8. Dwivedi, S. *Terminalia arjuna* Wight & Arn.-a useful drug for cardiovascular disorders. *J. Ethnopharmacol.***2007**,*114*, 114–129.
9. Pawar, R.S.; Bhutani, K.K. Effect of oleanane triterpenoids from *Terminalia arjuna*-a cardioprotective drug on the process of respiratory oxyburst. *Phytomedicine.* **2005**, *12*, 391-393.
10. Padma Sree, T. N.; Krishnakumar, S.; Senthilkumar, A.; Gopalakrishna, A.; Gummadi, S. N. *In vitro* Effect of *Terminalia arjunabark* extract on antioxidant enzyme catalase. *J.Pharmacol.Toxicol.***2007**, *2*, 698-708.
11. Manca,C.; Simon Paul, S.; Barry III, C.E.; Freedman, V.H.;Kaplan, G. *Mycobacterium tuberculosis*catalase and peroxidase activitiesand resistance to oxidative killing in humanmonocytes *in vitro*.*Infect. Immun.***1999**, *67*, 74–79.
12. Day Jr,W. A.;Sajecki,J. L.; Pitts,T. M.;Joens, L.A. Role of catalase in *Campylobacter jejuni*intracellular survival. *Infect. Immun.***2000**, *68*, 6337-6345.

13. Basu, M.; Czinn, S.J.; Blanchard, T.G. Absence of catalase reduces long-term survival of *Helicobacter pylori* in macrophage phagosomes. *Helicobacter*. **2004**, *9*, 211-216.
14. Newcomb, W.W.; Brown, J.C. Internal catalase protects Herpes Simplex virus from inactivation by hydrogen peroxide. *J. Virol.* **2012**, *86*, 11931–11934.
15. Roth, S.; Droge, W. Regulation of T cell growth factor (TCGF) production by hydrogen peroxide. *Cell. Immunol.* **1987**, *108*, 417-424.
16. Schreck, R.; Rieber, P.; Baeuerle, P. A. Reactive oxygen intermediates as apparently widely used messengers in the activation of the NF-kappaB transcription factor and HIV- 1. *EMBO J.* **1991**, *10*, 2247-2258.
17. Wu, F. A new coronavirus associated with human respiratory disease in China. *Nature*. **2020**, *579*, 265–269.
18. Novel Coronavirus (2019-nCoV) situation reports -116, 15May, **2020** <https://www.who.int/emergencies/diseases/novelcoronavirus-2019/situation-reports>.
19. Hua, Y. C.; Chun, C. C. L.; Ta, C. L. Anti-herpes simplex virus type 2 activity of casurinin from the bark of *Terminalia arjuna* Linn. *Antiviral Res.* **2002**, *55*, 447-455.
20. Justyna, P.; Moriola, B.S.; Ivana A. Study of the antioxidant properties of beers using electron paramagnetic resonance. *Food Chem.* **2013**, *141*, 3042-3049.
21. Ningijian, L.; David, D.K. Antioxidant property of coffee components: Assessment of methods that define mechanisms of action. *Molecules*. **2014**, *19*, 19181-19208.
22. Orhan, D.D.; Yeşilada, F.E.E.; Tsuchiya, K.; Takaishi, Y.; Kawazoe, K. Antioxidant activity of two flavonol glycosides from *Cirsium hypoleucum* DC through bioassay-guided fractionation. *Turkish J. Pharm. Sci.* **2007**, *41*, 1-14.

23. Zivkovic, J.; Zekovic, Z.; Music, I.; Tumbas, V.; Cvetkovic, D.; Spasojevic, I. Antioxidant properties of phenolics in *Castanea sativa* Mill. extracts. *Food Technol. Biotechnol.* **2009**, *47*, 421–427.
24. Sánchez, J.C.; Roberto Faure García, R.F.; Cors, M.T.M. 1,1-Diphenyl-2-picrylhydrazyl radical and superoxide anion scavenging activity of *Rhizophora mangle* (L.) bark. *Pharmacognosy Res.* **2010**, *2*, 279–284.
25. Ashby, E.C. Single-electron transfer, a major reaction pathway in organic chemistry. Answer to recent criticisms. *Acc. Chem. Res.* **1988**, *21*, 414–421.
26. Mader, E.A.; Davidson, E.R.; Mayer, J. M. Large ground-state entropy changes for hydrogen atom transfer reactions of iron complexes. *J. Am. Chem. Soc.* **2007**, *129*, 5153–5166.
27. Honda, T.; Miral, T.; Tsuyuki, T.; Takahashi, T.; Sawai, M. Chemical constituents from bark of *Terminalia arjuna*, *Bull. Chem. Soc. Japan.* **2001**, *49*, 3213–3225.
28. Sunyana, J.; Prem, P.Y.; Vikrant, G.; Neeru, V.; Neelam, S. *Terminalia arjuna* a sacred medicinal plant, phytochemical and pharmacological profile. *Phyto. Chem. Rev.* **2009**, *8*, 491–502.
29. Gauthaman, K.; Banerjee, S.K.; Dinda, A. K.; Ghosh, C.C.; Maulik, S.K. *Terminalia arjuna* (Roxb.) protects rabbit heart against ischemic-reperfusion injury: Role of antioxidant enzymes and heat shock protein. *J. Ethnopharmacol.* **2005**, *96*, 403–409.
30. Karthikeyan, B.R.; Sarala Bai, K.; Gauthaman, K.; Sathish, K.S.; Niranjali D.S. Cardioprotective effect of the alcoholic extract of *Terminalia arjuna* bark in an *in vivo* model of myocardial ischemic reperfusion injury. *Life Sciences.* **2003**, *73*, 2727–2739.
31. Leff, J. A.; Parsons, P. E.; Day, C. E.; Oppegard, M. A.; Moore, E. E.; Moore, F.; Repine, J. E. Increased hydrogen peroxide scavenging and catalase activity in serum from septic

- patients who subsequently develop the adult respiratory distress syndrome. *Am. Rev. Respir. Dis.* **1992**, *146*, 985-989.
32. Mani, J.S.; Johnson, J.B.; Steel, J.C.; Broszczak, D.A.; Neilsen, P.M.; Walsh, K.B.; Naiker, M. Natural product-derived phytochemicals as potential agents against coronaviruses: A review. *Virus Res.* **2020** Apr 30: 197989. doi: 10.1016/j.virusres.2020.197989
33. Stower, H. Lopinavir-titonavir in severe COVID-19. *Nat. Med.* **2020**, *26*, 465.
34. Manli, W.; Ruiyuan Cao.; Leike Z.; Xinglou, Y.; Jia, L; Mingyue, X.; Zhengli, S.; Zhihong, H.; Wu, Z.; Gengfu, X. Remdesvier and chloroquine effectively inhibit the recently emerged novel coronavirus (2019-nCoV) *in vitro*. *Cell Res.* **2020**, *30*, 269-271.
35. Moure, A.; Franco, D. J.; Sineiro, H.; Dominguez, M.; Nunez, M.J.; Lema, L.M. Antioxidant activity of extracts from *Gevuina avellana* and *Rosa rubiginosa* defatted seeds, *Food Res. Int.* **2001**, *34*, 103-109.
36. Adevaiton, B. D. S.; Dulce, H. S. S.; Vanderlan, S. B.; Luciana, A. S.; Tome, M. S.; Oswaldo, B. Antioxidant properties of plant extract; an EPR and DFT comparative study of the reaction with DPPH, TEMPOL and spin trap DMPO. *J. Braz. Chem. Soc.* **2009**, *20*, 1483-1492.

Potential of *Terminalia arjuna* as a Promising Phytoremedy Against COVID-19: DPPH Scavenging, Catalase Inhibition and Molecular Docking Studies

Department of Biotechnology, Bhupat and Jyoti Mehta School of Biosciences, Applied and Industrial Microbiology
Laboratory, Indian Institute of Technology Madras, Chennai, 600 036 India

*Corresponding author

Phone: (+91)-44-2257-4114, Fax: (+91)-44-2257-4102, Email: gummadi@iitm.ac.in

Supplementary Information

S.No.	Contents	Page No
Figure S1	Reaction mechanism of 2,2-diphenyl -1-picrylhydrazyl (DPPH) with ethanol extract	S3
Figure S2	Structures of compounds isolated from <i>T. arjuna</i> bark extract.	S4
Figure S3	ESI-MS spectrum of arjunetin isolated from ethanol extract	S5
Figure S4	ESI-MS mass spectral fragmentation analysis of arjunetin isolated from <i>T. arjuna</i> bark ethanol extract	S6
Figure S5	Schematic representation of extraction of various fractions from bark powder of <i>T.arjuna</i> .	S7
Figure S6	EPR spectrum of DPPH radical in ethanol	S8

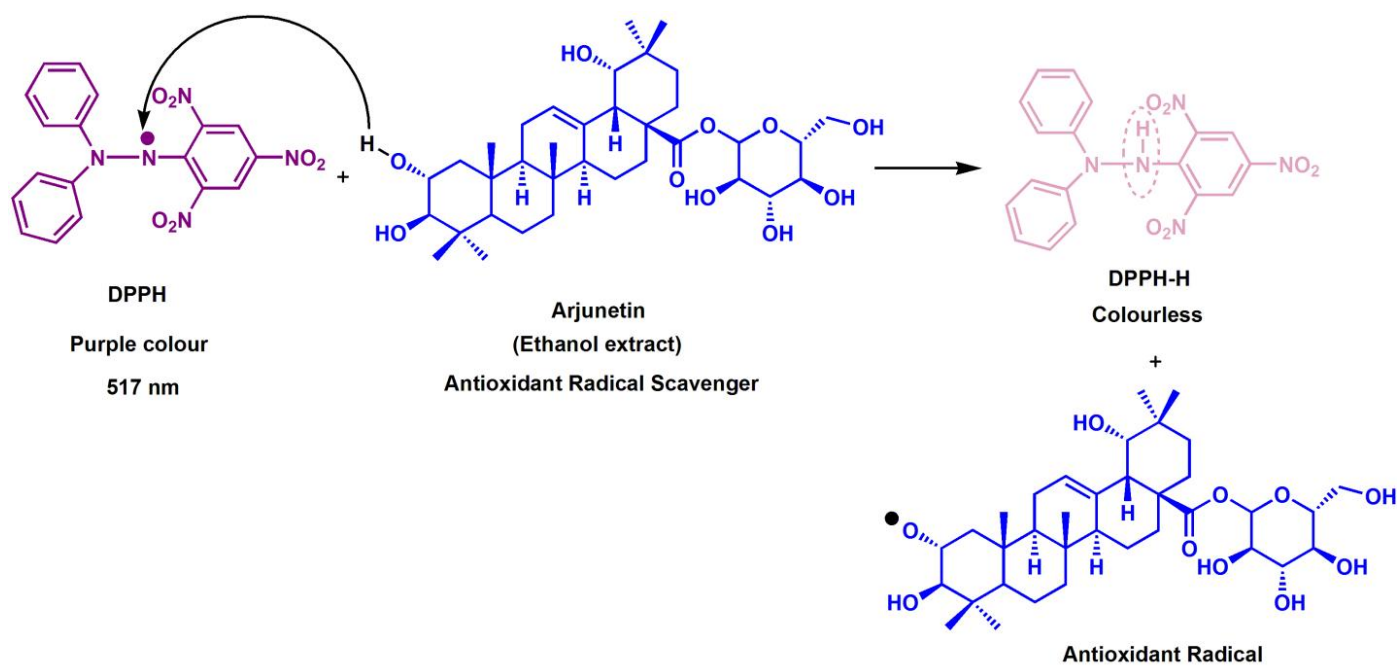


Figure S1: Reaction mechanism of 2,2-diphenyl -1-picrylhydrazyl (DPPH) with ethanol extract

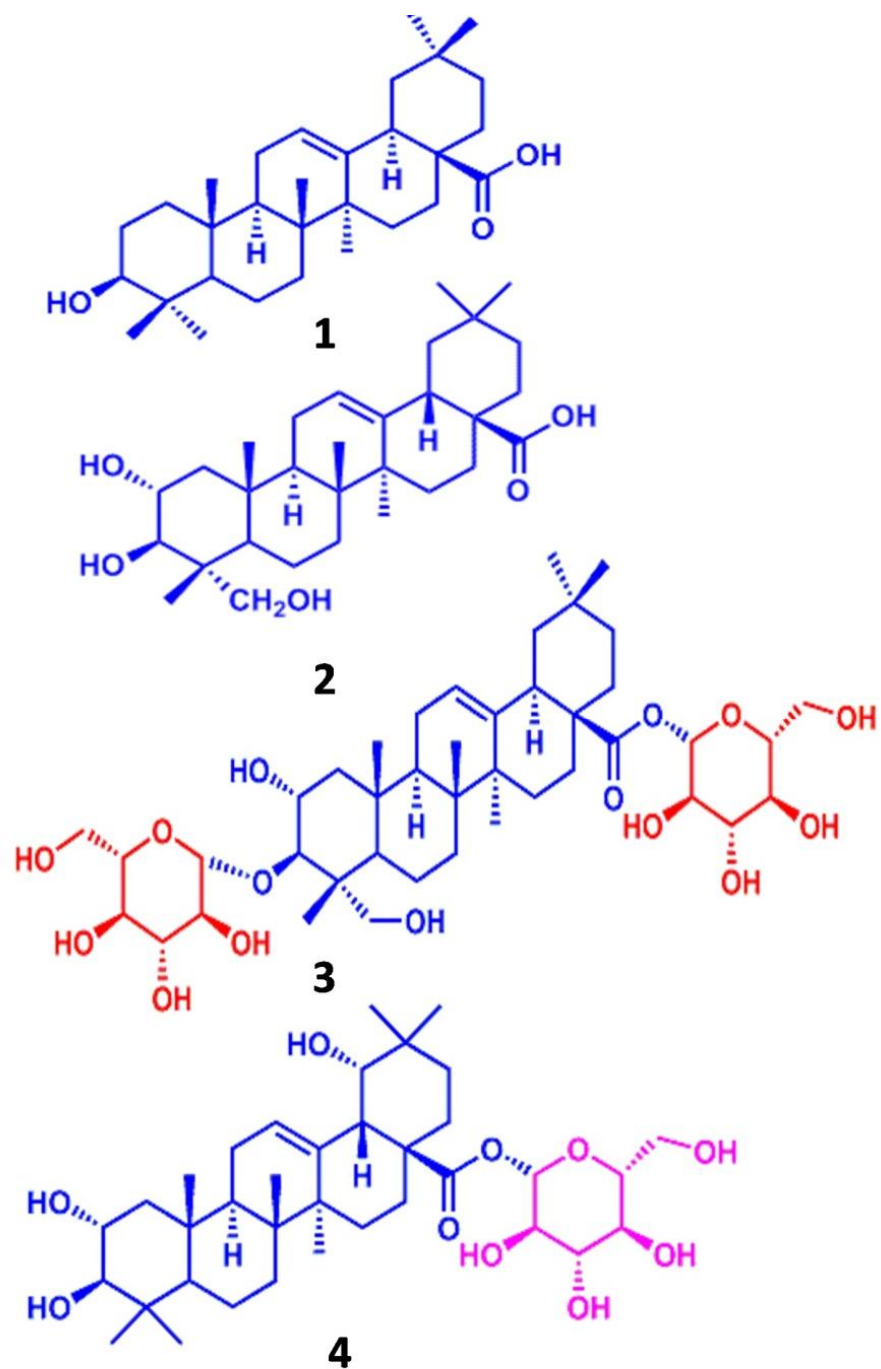


Figure S2: Structures of compounds isolated from *T. arjuna* bark extract.1. Oleanolic acid 2.Arjunolic acid 3.Arjunolitin 4.Arjunetin

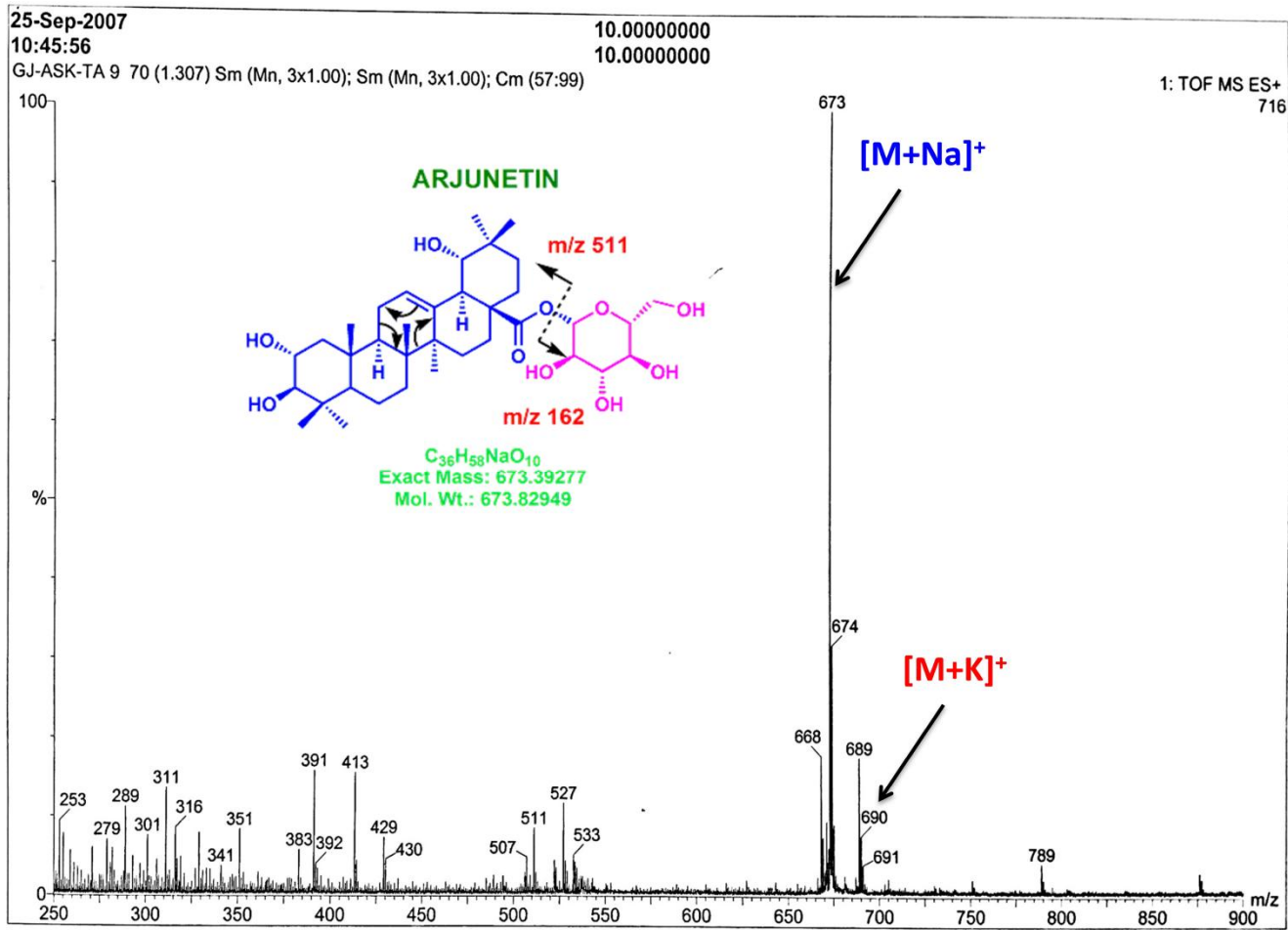


Figure S3: ESI-MS spectrum of arjunetin isolated from ethanol extract

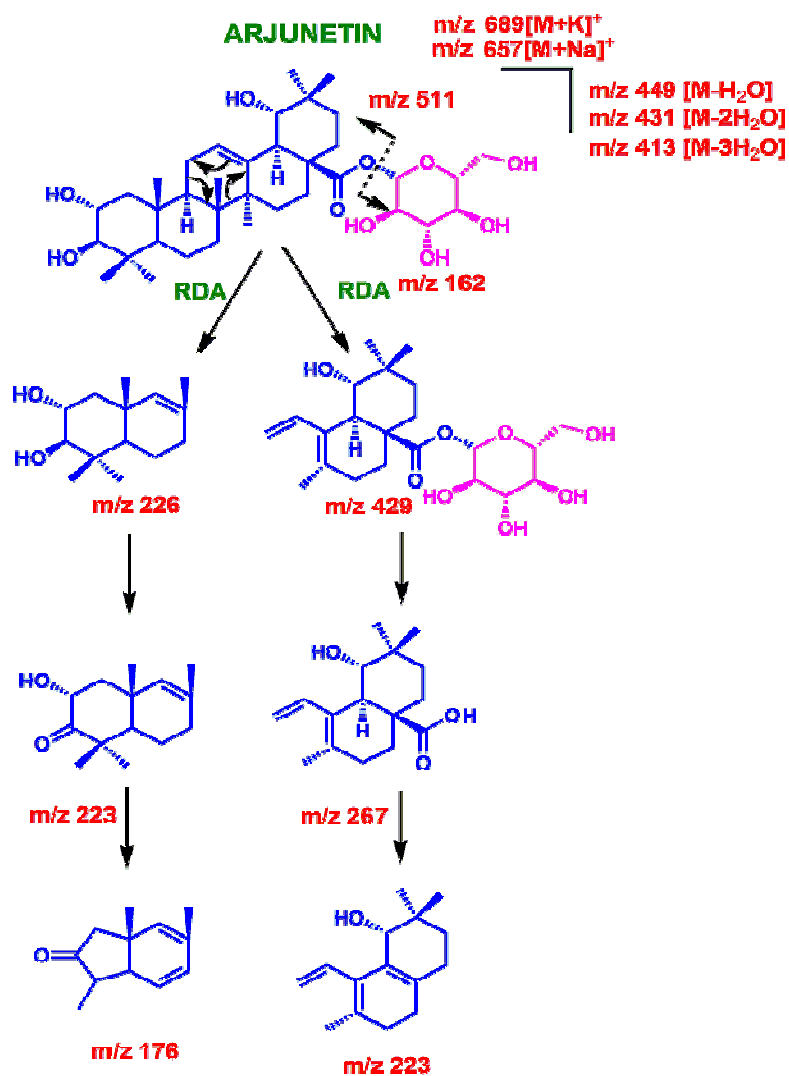


Figure S4: ESI-MS mass spectral fragmentation analysis of arjunetin isolated from *T. arjunabark* ethanol extract

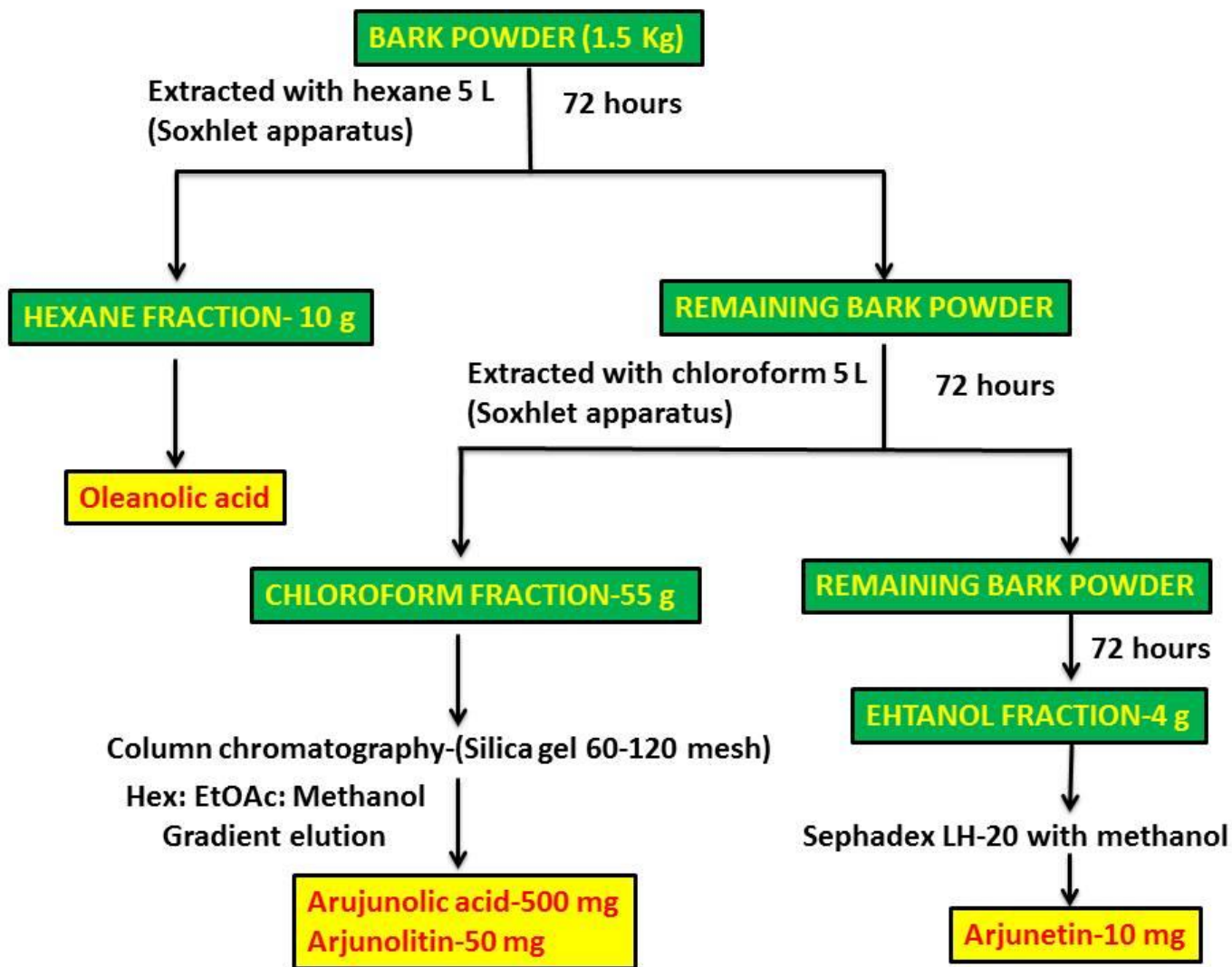


Figure S5: Schematic representation of extraction of various fractions from bark powder of *T.arjuna*.

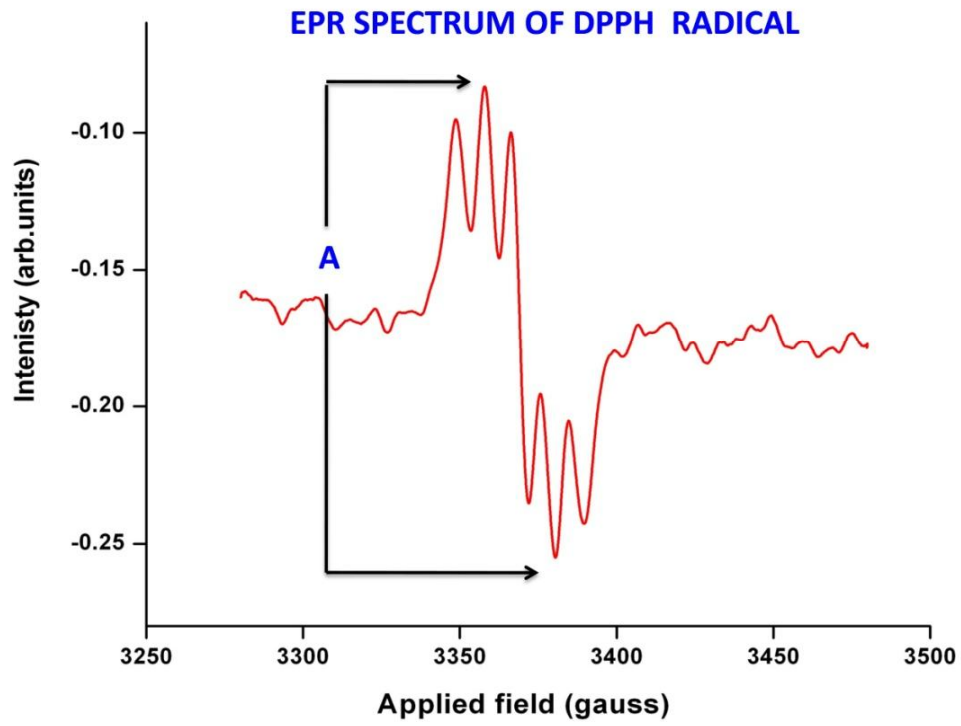


Figure S6: EPR spectrum of DPPH radical in ethanol